Quantification of the Impact of *GHG* Emissions on Unit Commitment in Microgrids

Ogun Yurdakul, Fikret Sivrikaya, and Sahin Albayrak
Department of Electrical Engineering and Computer Science
Technical University of Berlin, Berlin, Germany
Email: {yurdakul, fikret.sivrikaya, sahin.albayrak}@tu-berlin.de

***Abstract*—The global climate change creates a dire need to mitigate greenhouse gas (*GHG*) emissions from thermal generation resources (*TGR*s). While microgrids are instrumental in enabling the deeper penetration of renewable resources, the short-term planning of microgrids needs to explicitly assess the full range of impact of *GHG* emissions. To this end, we propose a novel unit commitment (*UC*) approach, which enables the representation of *GHG* emissions from *TGR*s, the specification of *GHG* emission constraints, and the ex-ante evaluation of carbon tax payment with all other costs and benefits. We quantify the relative merits of the proposed approach vis-à-vis the classical *UC* approach via representative studies. The results indicate that the proposed *UC* approach yields lower costs than does the classical *UC* approach and achieves a greater reduction in costs as carbon tax rate increases. Further, increasing carbon tax rates can markedly disincentivize *TGR* generation under the proposed approach.**

***Index Terms*—carbon tax, microgrids, power generation planning, unit commitment**

I. Introduction

A microgrid is a cluster of loads, distributed generation resources (*DGR*s), and electric storage resources (*ESR*s) that operate in coordination to supply electricity in a reliable manner. Typically integrated to its host power system at the distribution level, a microgrid is perceived by its distribution system as a single entity responding to appropriate signals [1]. For all intents and purposes, a microgrid is a microcosm of a bulk power system that retains most of its innate operational characteristics.

The *DGR*s in a microgrid can be broadly bifurcated into two categories: thermal generation resources (*TGR*s) and variable energy resources (*VER*s). *TGR*s include microturbines, fuel cells, and reciprocating internal combustion engines with generators and are especially common in microgrids in rural areas, developing nations, and military premises [2]. *TGR*s have controllable power output but can undergo only gradual temperature changes and hence are subject to minimum uptime, minimum downtime, and ramping constraints [3].

*VER*s, such as photovoltaic (*PV*) panels and wind turbines, are characterized by a renewable fuel source that can be neither stored nor controlled. *VER*s cannot be similarly situated to *TGR*s, since *VER* power outputs are highly time-varying, intermittent, and uncertain. Further, microgrids with integrated *ESR*s, such as batteries, ultracapacitors, and flywheels, possess various capabilities, including the hallmark capability to store electric energy for later use.

This work was supported in part by the Research Council of Norway under the "LUCS" project, and by the German Federal Ministry for Economic Affairs and Energy under Grant 03EI6004B.

Similar to bulk power systems, the short-term planning of a microgrid can be determined via unit commitment (*UC*) and economic dispatch (*ED*) decisions [4]. The classical unit commitment (*CUC*) approach seeks minimum cost strategies to determine the start-up and shut-down of *TGR*s based on expected load, equipment limitations, and operational policies [3]. The equipment limitations of *TGR*s and the inter-temporal constraints of microgrid physical asset operations render *UC* a time-coupled problem, and necessitate that the *UC* decisions be taken typically one-hour to one-week ahead of operations based on the uncertain data/information available at the time of decision. The injections levels of *TGR*s are subsequently determined by the solution of the *ED* problem after most of the uncertainty unravels.

Microgrids lend themselves as conducive environments to enabling the deeper penetration of *VER*s without unduly exacerbating the stress on transmission systems. As such, microgrids, aided by *UC* approaches that evaluate the full breadth of impact of greenhouse gas (*GHG*) emissions, can play a pivotal rule in combating global climate change.

The thorough assessment of *GHG* emissions in short-term microgrid operations hinges on practical *UC* approaches that expressly include *GHG* emission models. Such approaches further need to have the capability to stipulate explicit constraints on the amount of *GHG* emissions over a study period.

Another major requirement, brought on especially with the advent of carbon pricing schemes, is the analysis of the monetary impacts of *GHG* emissions. Carbon tax sets a specific price on the amount of emitted carbon dioxide equivalent (CO_2e) to internalize the negative externalities of *TGR* generation. The prevalence of carbon pricing has been soaring in recent years, with the price reaching $\$139/tCO_2e$ in Sweden [5].

The *CUC* approach does not consider *GHG* emissions and so does not take into account the carbon tax payment due to the *GHG* emissions from *TGR*s at the time of decision. As such, the carbon tax payment, for which the microgrid is liable, is evaluated *ex-post* under the *CUC* approach, thereby potentially bringing about dire economic implications. The *UC* approaches for microgrids must conduct an *ex-ante* evaluation of the carbon tax payment that will have been incurred, as per

Nomenclature

$\mathscr{H}$	set of simulation time periods
$\mathscr{G}$	set of distributed generation resources (*DGR*s)
$\mathscr{G}_{VER}$	set of variable energy resources (*VER*s)
$\mathscr{G}_{TGR}$	set of thermal generation resources (*TGR*s)
$\mathscr{S}$	set of electric storage resources (*ESR*s)
h	index of an hourly time period
γ_g	distributed generation resource g
σ_s	electric storage resource s
$[p^{\mathsf{i}}_{\gamma_g}]^m$	minimum power output of *DGR* γ_g (*kW*)
$[p^{\mathsf{i}}_{\gamma_g}]^M$	maximum power output of *DGR* γ_g (*kW*)
$[T^{\uparrow}_{\gamma_g}]^m$	minimum uptime of *TGR* γ_g (*hrs*)
$[T^{\downarrow}_{\gamma_g}]^m$	minimum downtime of *TGR* γ_g (*hrs*)
$\overline{\overline{c}}_{\gamma_g}$, $\overline{c}_{\gamma_g}$, c_{γ_g}	quadratic ($\$/kW^2h$), linear ($\$/kWh$), and fixed ($\$/h$) fuel cost parameter of *TGR* γ_g
μ_{γ_g}	start-up cost of *TGR* γ_g ($\$$)
$\overline{\overline{k}}_{\gamma_g}$, $\overline{k}_{\gamma_g}$, k_{γ_g}	quadratic ($kgCO_2e/kW^2h$), linear ($kgCO_2e/kWh$), and fixed ($kgCO_2e/h$) *GHG* emission parameter of *TGR* γ_g
$[\kappa]^M$	maximum *GHG* emission limit for the study period ($kgCO_2e$)
ψ	carbon tax rate ($\$/kgCO_2e$)
$\varkappa_{\gamma_g}$	*GHG* emissions of *TGR* γ_g over the study period ($kgCO_2e$)
κ	total *GHG* emissions from all microgrid *TGR*s over the study period ($kgCO_2e$)
$[p^{\mathsf{i}}_{\sigma_s}]^m$	minimum discharging power of *ESR* σ_s (*kW*)
$[p^{\mathsf{i}}_{\sigma_s}]^M$	maximum discharging power of *ESR* σ_s (*kW*)
$[p^{\mathsf{w}}_{\sigma_s}]^m$	minimum charging power of *ESR* σ_s (*kW*)
$[p^{\mathsf{w}}_{\sigma_s}]^M$	maximum charging power of *ESR* σ_s (*kW*)
$[E_{\sigma_s}]^m$	minimum energy storage limit of *ESR* σ_s (*kWh*)
$[E_{\sigma_s}]^M$	maximum energy storage limit of *ESR* σ_s (*kWh*)
$\eta^{\mathsf{i}}_{\sigma_s} \in (0,1]$	discharging efficiency of *ESR* σ_s
$\eta^{\mathsf{w}}_{\sigma_s} \in (0,1]$	charging efficiency of *ESR* σ_s
$p^{\mathsf{w}}_{\delta}[h]$	total microgrid load in hour h (*kW*)
$\lambda[h]$	the price at which the microgrid purchases (resp. sells) energy from (resp. to) the distribution company in hour h ($\$/kWh$)
$\big[R[h]\big]^m$	spinning reserve requirement for hour h (*kW*)
$p^{\mathsf{i}}_{\gamma_g}[h]$	power generation of *DGR* γ_g in hour h (*kW*)
$u^{\mathsf{i}}_{\gamma_g}[h]$	commitment status of *TGR* γ_g in hour h
$r^{\mathsf{i}}_{\gamma_g}[h]$	spinning reserve of *TGR* γ_g in hour h
$u^{\mathsf{i}}_{\sigma_s}[h]$	injection status of σ_s in hour h
$u^{\mathsf{w}}_{\sigma_s}[h]$	withdrawal status of σ_s in hour h
$p^{\mathsf{i}}_{\sigma_s}[h]$	power injection of σ_s in hour h (*kW*)
$p^{\mathsf{w}}_{\sigma_s}[h]$	power withdrawal of σ_s in hour h (*kW*)
$p^{\mathsf{n}}_{\sigma_s}[h]$	net power injection of σ_s in hour h (*kW*)
$E_{\sigma_s}[h]$	energy stored in σ_s in hour h (*kWh*)
$p^{\mathsf{n}}_{\varphi}[h]$	net power injection of the distribution system to the microgrid in hour h (*kW*)
$\xi^{\dagger}_{\gamma_g}$	fuel cost of *TGR* γ_g over the study period ($\$$)
$\xi^{\ddagger}_{\gamma_g}$	total start-up cost of *TGR* γ_g over the study period ($\$$)
ξ_{φ}	total net cost for the exchange of power with the distribution company ($\$$)
$\xi_{\varkappa}$	carbon tax payment ($\$$)

the effective carbon pricing schemes. The ex-ante evaluation of carbon tax payment permits a more thorough quantification of the benefits of taking *UC* decisions that favor the greater utilization of *VER*s jointly with *ESR*s in lieu of *TGR*s.

While economic mechanisms can serve as prime movers for major change, a key issue that needs to be investigated is whether carbon tax rates can effectively deter the use of *TGR*s and incentivize the further utilization of *VER*s in conjunction with *ESR*s. As such, the analytical study of the influence of carbon pricing schemes on *UC* decisions can provide useful guidance for policy makers addressing global warming.

A. Related Work

There is a growing body of literature on *UC* approaches for microgrids. In [4], the authors propose a *UC* approach for microgrids with integrated *TGR*s, *VER*s, and *ESR*s, yet the proposed approach does not consider the *GHG* emissions from integrated *TGR*s or evaluate the monetary impacts of *GHG* emissions. The frameworks presented in [6], [7] consider *ESR*s, *TGR*s, and *VER*s in the *UC* of a microgrid; nonetheless, they do not model the *GHG* emissions from *TGR*s or their economic implications.

In [8], the *UC* decisions for microgrids with integrated *TGR*s and *VER*s have been studied, where the *GHG* emissions from *TGR*s are modeled. However, [8] does not include an explicit constraint on the amount of *GHG* emissions, study carbon tax rates, or include *ESR*s—which are key to enable the greater utilization of *VER*s and so to mitigate *GHG* emissions. While the approach presented in [9] models the *GHG* emissions from *TGR*s of a microgrid, it does not impose any constraints on the amount of *GHG* emissions or evaluate the impact of carbon tax rates. In [10], the *UC* of a microgrid is studied, where the *GHG* emissions from *TGR*s and carbon emission costs are modeled. However, the authors of [10] do not study the influence of carbon tax rate on *UC* decisions or model an explicit constraint for *GHG* emissions from *TGR*s in the *UC* problem formulation.

B. Contributions of the paper

The general contributions and novel aspects of this paper are as follows:

1) We propose a novel *UC* approach that comprehensively evaluates the full range of impact of *GHG* emissions. We refer to this approach as *environmental unit commitment* or *EUC*. To the best of our knowledge, this is the first approach that simultaneously models *GHG* emissions, allows the stipulation of a constraint on *GHG* emission amount, and conducts an ex-ante evaluation of the carbon tax payment. We conduct representative studies and demonstrate the effectiveness of the proposed *EUC* approach on real-world data.
2) We examine the sensitivity of the *UC* decisions to carbon tax rate and study the extent to which carbon tax can influence the operation of microgrid *TGR*s, *ESR*s, and power exchange with the distribution grid. Our findings regarding the influence of carbon tax rate on short-

term microgrid operations could prove useful for policy makers in judiciously determining carbon tax rate.

This paper contains four additional sections. In Section II, we develop models for the microgrid physical, economic, and environmental aspects. In Section III, we present the mathematical formulations of the *EUC* and *CUC* approaches. We illustrate the capabilities and effectiveness of the proposed *EUC* approach in Section IV with representative studies and discuss the results. We summarize the paper and provide directions for future work in Section V.

This column is intentionally left blank.

II. Microgrid Modeling

We devote this section to the delineation of the microgrid models. We discretize the time axis and adopt one hour as the smallest indecomposable unit of time. In line with [11], we decompose the study period into H non-overlapping hours and define the study period by the set $\mathscr{H} := \{h\colon h = 1, ..., H\}$.

A. Physical Asset Models

We consider a microgrid interfaced with the distribution system and denote by $\mathscr{G}$ the set of *DGR*s in the microgrid. We define the subsets $\mathscr{G}_{VER}$ and $\mathscr{G}_{TGR}$ to denote the set of *VER*s and *TGR*s, respectively, and we write the relation $\mathscr{G} = \mathscr{G}_{VER} \bigcup \mathscr{G}_{TGR}$. We define by $p^{\mathsf{i}}_{\gamma_g}[h]$ the *kW* power injection of $\gamma_g \in \mathscr{G}$ in hour h.

The binary variable $u^{\mathsf{i}}_{\gamma_g}[h] \in \{0, 1\}$ denotes the commitment status of *TGR* $\gamma_g \in \mathscr{G}_{TGR}$ in hour h. $u^{\mathsf{i}}_{\gamma_g}[h] = 1$ if γ_g is up in hour h, and 0 otherwise. We define by $r^{\mathsf{i}}_{\gamma_g}[h]$ the spinning reserve of *TGR* $\gamma_g \in \mathscr{G}_{TGR}$ in hour h. We denote by $p^{\mathsf{w}}_{\delta}[h]$ the total *kW* load of the microgrid in hour h.

We model the load of the microgrid over the study period by the random vector $\tilde{\boldsymbol{\ell}} = (\tilde{\ell}_1, \ldots, \tilde{\ell}_h, \ldots, \tilde{\ell}_{24})$, where $\tilde{\ell}_h$ is the random variable representing the uncertain load in hour h. We assume that $\tilde{\boldsymbol{\ell}}$ is a Gaussian random vector, i.e., $\tilde{\boldsymbol{\ell}} \sim \mathcal{N}(\boldsymbol{\mu}, \boldsymbol{K})$ with mean vector $\boldsymbol{\mu}$ and the covariance matrix $\boldsymbol{K}$. As such, the random variables are jointly Gaussian and thus independent, rendering $\boldsymbol{K}$ a diagonal matrix with $Cov(\tilde{\ell}_i, \tilde{\ell}_j) = 0$ for $i \neq j$.

B. Economic Models

In this subsection, we model the costs and benefits associated with the microgrid operation over the study period. We express the fuel cost of *TGR* γ_g over the study period by

$$\xi_{\gamma_g} = \sum_{h \in \mathscr{H}} \Big[\big(\bar{c}_{\gamma_g}(p^{\mathsf{i}}_{\gamma_g}[h]) + c_{\gamma_g} u^{\mathsf{i}}_{\gamma_g}[h] \big)(1\ hr) \Big], \tag{1}$$

based on [4]. We consider that the microgrid has the capability to purchase power through a forward contract that must be rolled out ahead of power dispatch, i.e., before the realization of uncertain load values. The purchased power stipulated for each hour in the forward contract must be purchased during its corresponding time period, even if it may not be needed to meet the load. We denote by $p^{\mathsf{i}}_{\dagger}[h]$ the power purchased through the forward contract for hour h and by $\lambda_{\dagger}[h]$ the price of energy stipulated in the forward contract for hour h. We express the total cost for energy purchased through the forward contract by:

$$\xi_{\dagger} = \sum_{h \in \mathscr{H}} \Big[\lambda_{\dagger}[h] p^{\mathsf{i}}_{\dagger}[h] (1\ hr) \Big]. \tag{2}$$

We further assume that the microgrid has the capability to purchase power in real time after uncertain net load values get revealed. We denote by $p^{\mathsf{i}}_{\ddagger}[h]$ the power purchased in real time in hour h and by $\lambda_{\ddagger}[h]$ the price of energy purchased real in time in hour h. We state the total cost for energy purchased in real time by:

$$\xi_{\ddagger} = \sum_{h \in \mathscr{H}} \Big[\lambda_{\ddagger}[h] p^{\mathsf{i}}_{\ddagger}[h] (1hr) \Big]. \tag{3}$$

III. Stochastic Unit Commitment Problem Formulation

In this section, we present the stochastic unit commitment problem formulation using the physical asset models and economic models developed in Section II. The devised problem relies on a two-stage stochastic formulation, where the decisions for the first-stage problem are the unit commitment statuses ($u^{\mathsf{i}}_{\gamma_g}[h]$) and the power purchased through the forward contract ($p^{\mathsf{i}}_{\dagger}[h]$), which are *here-and-now* decisions taken before the uncertain load values get revealed. We succinctly express the first-stage variables by the vector $\boldsymbol{x}$, which comprises $u^{\mathsf{i}}_{\gamma_g}[h]$ and $p^{\mathsf{i}}_{\dagger}[h]$. The first-stage problem is stated as:

$$\underset{u^{\mathsf{i}}_{\gamma_g}[h], p^{\mathsf{i}}_{\dagger}[h]}{\text{minimize}} \Bigg\{ \sum_{h \in \mathscr{H}} \big[c_{\gamma_g} u^{\mathsf{i}}_{\gamma_g}[h] + \lambda_{\dagger}[h] p^{\mathsf{i}}_{\dagger}[h] \big] + \mathbb{E}\big[F(\boldsymbol{x}, \tilde{\boldsymbol{\ell}}) \big] \Bigg\} \tag{4}$$

subject to

$$u^{\mathsf{i}}_{\gamma_g}[h] \in \{0, 1\} \quad \forall \gamma_g \in \mathscr{G},\ \forall h \in \mathscr{H}, \tag{5}$$

$$p^{\mathsf{i}}_{\dagger}[h] \geq 0 \quad \forall h \in \mathscr{H}, \tag{6}$$

where $F(\boldsymbol{x}, \tilde{\boldsymbol{\ell}})$ represents the uncertain second-stage costs. For first-stage decisions $(u^{\mathsf{i}}_{\gamma_g}[h])^{\star}$ and $(p^{\mathsf{i}}_{\dagger}[h])^{\star}$ and a specific realization ω of load $\boldsymbol{\ell^{\omega}}$, $F(\boldsymbol{x}^{\star}, \boldsymbol{\ell^{\omega}})$ is obtained by solving the following second-stage problem:

$$F(\boldsymbol{x}^{\star}, \boldsymbol{\ell^{\omega}}) := \underset{p^{\mathsf{i}}_{\gamma_g}[h], p^{\mathsf{i}}_{\ddagger}[h]}{\text{minimize}} \sum_{h \in \mathscr{H}} \Big[\bar{c}_{\gamma_g} p^{\mathsf{i}}_{\gamma_g}[h] + \lambda_{\ddagger}[h] p^{\mathsf{i}}_{\ddagger}[h] \Big] \tag{7}$$

subject to

$$(u^{\mathsf{i}}_{\gamma_g}[h])^{\star} [p^{\mathsf{i}}_{\gamma_g}]^{m} \leq p^{\mathsf{i}}_{\gamma_g}[h] \leq (u^{\mathsf{i}}_{\gamma_g}[h])^{\star} [p^{\mathsf{i}}_{\gamma_g}]^{M} \quad \forall \gamma_g \in \mathscr{G}\ \forall h \in \mathscr{H}, \tag{8}$$

$$\sum_{\gamma_g \in \mathscr{G}} p^{\mathsf{i}}_{\gamma_g}[h] + (p^{\mathsf{i}}_{\dagger}[h])^{\star} + p^{\mathsf{i}}_{\ddagger}[h] \geq \ell^{\omega}_{h} \quad \forall h \in \mathscr{H}, \tag{9}$$

$$p^{\mathsf{i}}_{\ddagger}[h] \geq 0 \quad \forall h \in \mathscr{H}. \tag{10}$$

The power dispatch of the *TGR*s ($p^{\mathsf{i}}_{\gamma_g}[h]$) and the power purchased in real time ($p^{\mathsf{i}}_{\ddagger}[h]$) are *wait-and-see* decisions that are taken after the uncertain load values are realized.

Suppose, we draw $\mathcal{N}$ crude Monte Carlo samples of the uncertain load vector $\tilde{\boldsymbol{\ell}}$, *viz.*, $\boldsymbol{\ell^{1}}, \ldots, \boldsymbol{\ell^{\omega}}, \ldots, \boldsymbol{\ell^{\mathcal{N}}}$. Using sample average approximation (*SAA*), we recast the first-stage problem as follows:

$$\underset{u^{\mathsf{i}}_{\gamma_g}[h], p^{\mathsf{i}}_{\dagger}[h]}{\text{minimize}} \Bigg\{ \sum_{h \in \mathscr{H}} \big[c_{\gamma_g} u^{\mathsf{i}}_{\gamma_g}[h] + \lambda_{\dagger}[h] p^{\mathsf{i}}_{\dagger}[h] \big] + \frac{1}{\mathcal{N}} \big[F(\boldsymbol{x}, \boldsymbol{\ell^{\omega}}) \big] \Bigg\} \tag{11}$$

subject to

$$u^{\mathsf{i}}_{\gamma_g}[h] \in \{0, 1\} \quad \forall \gamma_g \in \mathscr{G},\ \forall h \in \mathscr{H}, \tag{12}$$

$$p^{\mathsf{i}}_{\dagger}[h] \geq 0 \quad \forall h \in \mathscr{H}. \tag{13}$$

IV. Case Study and Results

In this section, we illustrate the application and effectiveness of the proposed *EUC* approach on representative studies.

A. Case Study Data

We consider a microgrid connected to the low-voltage side of the distribution transformer to power residential loads. We consider that the microgrid includes a diesel generator denoted by γ_1, a *PV* panel denoted by γ_2, and an *ESR* denoted by σ_1. The peak load of the microgrid is 37 *kW*.

The γ_1 has a peak capacity of 50 *kW*. The γ_1 cost parameters are $\overline{\overline{c}}_{\gamma_1} = \$1.20(10^{-3})/kW^2h$, $\overline{c}_{\gamma_1} = \$0.208/kWh$, and $c_{\gamma_1} = \$3.2/h$. Further, the γ_1 *GHG* emission parameters are $\overline{\overline{k}}_{\gamma_1} = 3.03(10^{-3})\,kgCO_2e/kW^2h$, $\overline{k}_{\gamma_1} = 0.53\,kgCO_2e/kWh$, and $k_{\gamma_1} = 8.09\,kgCO_2e/h$. The data for γ_1 and σ_1 are extracted from [4], [12] and presented in Table I. The peak capacity of σ_2 is 17 *kW*. The load and *PV* generation data are extracted from [13] and contain measurements for an anonymous house in New York. Since the load and *PV* data are collected in New York, to ensure consistency, we consider the time-of-use rates offered by Con Edison, *viz.*: 21.97*¢/kWh* from 8 a.m. to midnight and 1.55*¢/kWh* from midnight to 8 a.m. [14]. We consider a 15% minimum reserve requirement measured with respect to the microgrid peak load over the study period provided solely by *TGR* γ_1. We explicitly stipulate a constraint on the allowable *GHG* emissions over the study period and take $[\kappa]^M = 220\,kgCO_2e$. We further consider that the carbon tax rate is $\psi = \$0.07/kgCO_2e$.

TABLE I
Case study data for *TGR* γ_1 and *ESR* σ_1

parameter	value	parameter	value	parameter	value
$[p^{\mathrm{i}}_{\gamma_1}]^m$	5 *kW*	$[p^{\mathrm{i}}_{\gamma_1}]^M$	50 *kW*	μ_{γ_1}	\$1
$[T^{\uparrow}_{\gamma_1}]^m$	2 *hrs*	$[T^{\downarrow}_{\gamma_1}]^M$	2 *hrs*	$u^{\mathrm{i}}_{\gamma_1}[0]$	0
$[p^{\mathrm{i}}_{\sigma_1}]^m$	0 *kW*	$[p^{\mathrm{w}}_{\sigma_1}]^m$	0 *kW*	$[E_{\sigma_1}]^m$	0 *kWh*
$[p^{\mathrm{i}}_{\sigma_1}]^M$	12 *kW*	$[p^{\mathrm{w}}_{\sigma_1}]^M$	12 *kW*	$[E_{\sigma_1}]^M$	30 *kWh*

B. Load and PV Forecasting

The computation of the numerical solutions of the *EUC* and *CUC* problems requires the numerical representation of *VER* generation and microgrid load over the study period. To this end, in this section, we utilize the methodology presented in [15] to forecast *PV* generation and microgrid load over the study period. The utilized methodology leverages a sequence-to-sequence (*S2S*) architecture that comprises two long short-term memory (*LSTM*) networks, *viz.*: encoder and decoder.

We construct one *S2S* architecture for each of the two forecasting tasks. We provide each *S2S* architecture with the measurements for the previous 24 hours as well as the hour of the day and the day of the week of the forecasted time periods. Further, each *S2S* architecture generates forecasts for the subsequent 24 hours. It is worth emphasizing that, since the data in [13] were anonymized and the exact location of the house was not disclosed, we did not provide the *S2S* architectures with relevant weather data, such as cloudiness index or temperature. Nevertheless, different studies can utilize other forecasting methodologies, probability distributions, or historical data in the implementation of the *EUC* approach.

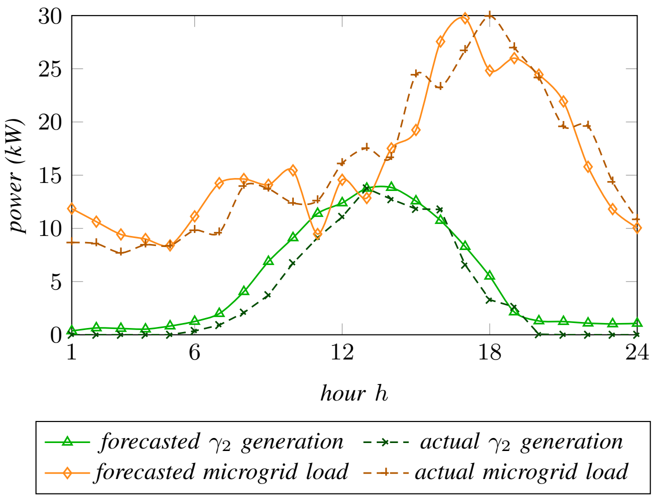

Fig. 1. Forecasted and actual γ_2 generation and microgrid load

The dataset of each *S2S* architecture contains measurements collected between May 1, 2019 and July 29, 2019 at one-hour resolution. Each dataset is split into training (60%), validation (20%), and test (20%) sets, and we use the validation sets to tune the hyperparameters of the *S2S* architectures. We pick the date of July 29, 2019 as the study period. The values for July 28, 2019 and July 29, 2019 are in the test set; therefore, the *S2S* architectures have not been trained with the specific study period or the preceding day values. We utilize Tensorflow and Keras to train, validate, and test the *S2S* architectures on an NVIDIA Tesla P100 16 *GB GPU* with 800 *GB* of *RAM*.

The *S2S* architecture to forecast *PV* generation contains one *LSTM* layer comprising 512 *LSTM* blocks in both the encoder and decoder networks. We use the *Adam* optimizer, and to prevent the networks from overfitting, utilize dropout with a probability of 0.4. The *S2S* architecture to forecast *PV* generation yields an *RMSE* of 0.2876 on the test set.

The *S2S* architecture to forecast microgrid load has one *LSTM* layer comprising 512 *LSTM* blocks in the encoder network and two *LSTM* layers each comprising 512 *LSTM* blocks in the decoder network. We pick *Adam* as the optimizer and use dropout with a probability of 0.5. The *S2S* architecture to forecast the microgrid load achieves an *RMSE* of 0.5825 on the test set. Fig. 1 depicts the *S2S* architecture forecasts for the study period along with the corresponding actual measurements. The *S2S* architecture forecasts for July 29, 2019 are utilized in the *EUC* and *CUC* solutions to represent γ_2 generation and microgrid load over the study period.

C. Unit Commitment Results

The *EUC* problem formulation described by (**??**)-(**??**) is a mixed-integer-programming (*MIP*) problem known to be *NP*-hard. We solve the *EUC* problem using Gurobi 8.1 on a 2.6

GHz Intel Core i7 *CPU* with 16 *GB* of *RAM* for the study period. Fig. 2 presents the optimal injections and withdrawals under the *EUC* and *CUC* approaches. In both formulations, σ_1 tends to charge (resp. discharge) when the *DisCo* electricity rates are low (resp. high), thereby exploiting intraday price variation and capitalizing on arbitrage opportunities.

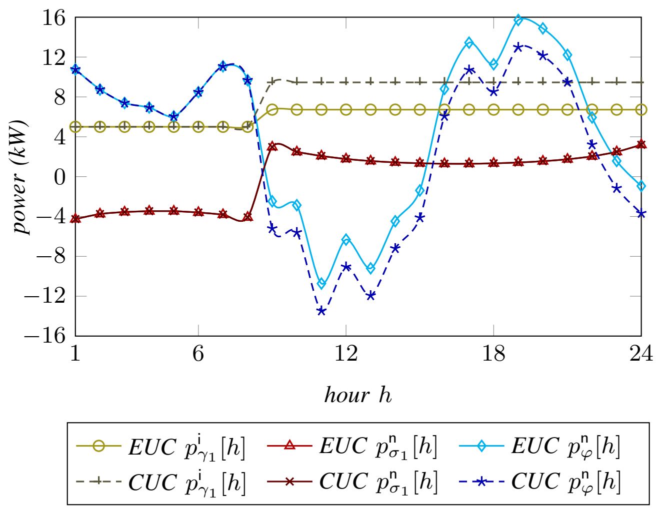

Fig. 2. Optimal operations under the *EUC* and *CUC* approaches

The marked difference between the *EUC* and *CUC* approaches manifests itself in the optimal operations from hour 9 to hour 24. The optimal *EUC* solution generates less energy from the *TGR* compared to the optimal *CUC* solution, since the *EUC* approach is cognizant of the carbon tax payment while taking *UC* decisions. On the flip side, the *CUC* approach does not consider the carbon tax payment while taking *UC* decisions and so needs to conduct an ex-post evaluation of the carbon tax payment for which the microgrid is liable. Owing to this ex-ante evaluation of carbon tax payment, the total costs for the study period are 16.9¢ lower under the *EUC* approach than those under the *CUC* approach.

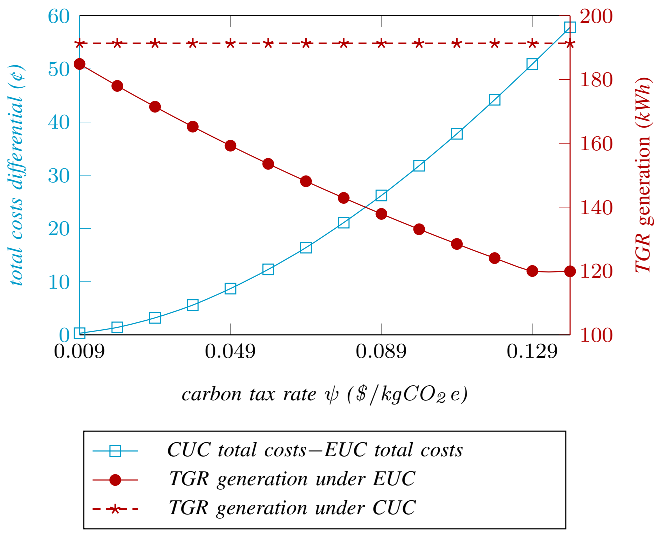

Fig. 3. Influence of carbon tax rate on the *EUC* and *CUC* approaches

While the simulation depicted in Fig. 2 is performed for the specific carbon tax rate $\psi = \$0.07/kgCO_2e$, we also would like to examine the influence of the carbon tax rate on the quantifiable benefits of the *EUC* approach. To this end, we study the sensitivity of the total costs to changes in the carbon tax rate. We vary the carbon tax rate ψ from $\$0.009/kgCO_2e$ to the highest global carbon tax rate in 2018 of $\$0.139/kgCO_2e$ implemented in Sweden, in $\$0.010/kgCO_2e$ increments.

Fig. 3 illustrates the energy generation from the *TGR* γ_1 over the study period under the *EUC* and *CUC* approaches, as a function of ψ. Under *EUC* approach, while the lowest simulated carbon tax rate resulted in a *TGR* generation of 184.86 *kWh*, the highest simulated carbon tax rate resulted in a significantly lower *TGR* generation of 120 *kWh*. The *TGR* generation under the *CUC* approach, however, does not vary with carbon tax rate and attains the constant value of 191.33 *kWh*, because the *CUC* approach does not consider the impact of carbon tax rate at the time of decision. The plots make clear that the carbon tax rate can effectively disincentivize *TGR* generation under the *EUC* approach in comparison with the *CUC* solution.

Fig. 3 also presents the difference between the total costs obtained by the *EUC* and *CUC* approaches, *i.e.*, the total costs under the *CUC* approach minus the total costs under the *EUC* approach, as a function of ψ. The results indicate that, for all considered carbon tax rates, the total costs under the *EUC* approach are lower than those under the *CUC* approach. We further observe that, as ψ increases, the reduction in total costs under the *EUC* approach vis-à-vis the *CUC* approach also increases. This observation can be attributed to the fact that the *EUC* approach optimizes the microgrid operation by taking into account the carbon tax payment based on varying carbon tax rates. The *CUC* approach, however, can only evaluate the impact of increasing carbon tax rate ex-post, which inevitably results in higher costs with increasing carbon tax rates. These results underscore the importance of the explicit consideration of the monetary impacts of *GHG* emissions by *UC* approaches.

V. Conclusion

In this paper, we propose a *UC* approach that expressly assesses the *GHG* emissions from *TGR*s as well as their monetary impacts. The proposed *EUC* approach enables the stipulation of a constraint on *GHG* emissions from *TGR*s over the study period and the ex-ante evaluation of carbon tax payment jointly with all other costs and benefits. The results indicate that the proposed approach yields lower costs than does the classical *UC* approach. Further, it was observed that the *TGR* operation could be attenuated via an economic mechanism, *i.e.*, carbon tax rate, when the carbon tax payment is ex-ante evaluated. The performed sensitivity analysis provides valuable insights into the impact of carbon tax rate on the *EUC* and *CUC* approaches.

In our future studies, we plan to incorporate emissions trading schemes to the proposed *EUC* approach. To evaluate a wider range of costs and benefits, we further plan to represent the participation of microgrids in wholesale energy and ancillary services markets under the *EUC* approach.

References

[1] D. E. Olivares *et al.*, "Trends in microgrid control," *IEEE Transactions on Smart Grid*, vol. 5, no. 4, pp. 1905–1919, 2014.

[2] J. D. Glover, M. S. Sarma, and T. Overbye, *Power System Analysis and Design*, 5th ed. Stamford, CT: Cengage Learning, 2012, p. 32.

[3] A. J. Wood, B. F. Wollenberg, and G. B. Sheblé, *Power Generation, Operation and Control*, 3rd ed., Hoboken, NJ, 2014, pp. 148–153.

[4] T. A. Nguyen and M. L. Crow, "Stochastic optimization of renewable-based microgrid operation incorporating battery operating cost," *IEEE Transactions on Power Systems*, vol. 31, no. 3, pp. 2289–2296, May 2016.

[5] "State and trends of carbon pricing 2018," Tech. Rep., May 2018. [Online]. Available: https://openknowledge.worldbank.org/handle/10986/29687

[6] X. Wu, X. Wang, and C. Qu, "A hierarchical framework for generation scheduling of microgrids," *IEEE Transactions on Power Delivery*, vol. 29, no. 6, pp. 2448–2457, Dec 2014.

[7] A. Solanki, A. Nasiri, V. Bhavaraju, Y. L. Familiant, and Q. Fu, "A new framework for microgrid management: Virtual droop control," *IEEE Transactions on Smart Grid*, vol. 7, no. 2, pp. 554–566, March 2016.

[8] F. Li, J. Qin, and Y. Kang, "Closed-loop hierarchical operation for optimal unit commitment and dispatch in microgrids: A hybrid system approach," *IEEE Transactions on Power Systems*, vol. 35, no. 1, pp. 516–526, Jan 2020.

[9] V. Sarfi, I. Niazazari, and H. Livani, "Multiobjective fireworks optimization framework for economic emission dispatch in microgrids," in *2016 North American Power Symposium (NAPS)*, Sep. 2016, pp. 1–6.

[10] Z. Ding and W. Lee, "A stochastic microgrid operation scheme to balance between system reliability and greenhouse gas emission," in *2015 IEEE/IAS 51st Industrial Commercial Power Systems Technical Conference (I CPS)*, 2015, pp. 1–9.

[11] O. Yurdakul, "Analysis and performance evaluation of coordinated transaction scheduling," M.S. thesis, University of Illinois at Urbana-Champaign, Urbana, IL, 2018. [Online]. Available: http://hdl.handle.net/2142/101097

[12] S. Greene and A. Lewis, "Global Logistics Emissions Council Framework for Logistics Emissions Accounting and Reporting," Tech. Rep., 2019. [Online]. Available: https://www.inlandwaterwaytransport.eu/wp-content/uploads/2019GLECFramework_Aug2019.pdf

[13] Pecan Street Inc., "Dataport," December 2019. [Online]. Available: https://dataport.pecanstreet.org

[14] Consolidated Edison Company of New York, Inc. (2019) Time-of-Use Rates. [Online]. Available: https://www.coned.com/en/save-money/energy-saving-programs/time-of-use

[15] D. L. Marino, K. Amarasinghe, and M. Manic, "Building energy load forecasting using deep neural networks," in *IECON 2016 - 42nd Annual Conference of the IEEE Industrial Electronics Society*, Oct 2016, pp. 7046–7051.